

Comparative Analysis of the Brillouin Frequency Shift Determining Accuracy in Extremely Noised Spectra by Various Correlation Methods

A. I. Krivosheev^{a,*}, Yu. A. Konstantinov^a, F. L. Barkov^c, and V. P. Pervadchuk^b

^aPerm Federal Research Center of the Ural Branch of the Russian Academy of Sciences,
Perm, 614990 Russia

^bPerm National Research Polytechnic University,
Perm, 614990 Russia

^cOptical reflectometry, metrology and sensing International Conference Program Committee,
Perm, 614990 Russia

*e-mail: antokri@ya.ru

Received March 24, 2021; revised April 23, 2021; accepted April 26, 2021

Abstract—Using the same extremely noised data, two correlation methods for finding the maxima of Brillouin spectra are compared. The first method is a well-known method of correlating the received signal with the ideal Lorentzian function. In the second method, developed by the authors earlier, instead of the Lorentzian function, the same spectrum under study, but inverted along the frequency axis, is used (Backward correlation method, BWC). In addition to evaluating the accuracy of both methods, they are compared with the classical method of Lorentzian curve fitting. The accuracy of the considered methods is estimated depending on the probability of artefacts appearing in the Brillouin scattering spectra. It is shown that when the 9% probability of the artifact occurrence is exceeded, the BWC method shows better results than the other methods considered.

DOI: 10.1134/S0020441221050067

INTRODUCTION

Distributed fiber-optic sensors have found their application in solving a wide range of scientific and technical problems. In general, their principle of operation is based on the registration of various components of backscattering at each point of the optical fiber and the study of its spectral, phase, polarization and other properties using mathematical signal processing. Recently, distributed sensors based on stimulated and spontaneous Brillouin scattering, operating on the principle of light scattering on an acoustic phonon present in the propagation medium, i.e. in an optical fiber, have become widespread. Temperature and deformation effects change the speed of sound in the quartz glass, the material the fiber is made of, which leads to a frequency shift of the ultra-weak spectral components of backscattering. In this case, the main desired value is the frequency of the spectral component maximum (BFS—Brillouin Frequency Shift). After the initial analog-to-digital conversion, the registered spectra are discrete functions containing digital electrical noise, in which the desired spectral component, which is the Lorentzian function, is often hard to be found. Simple finding a local maximum in

extremely noised signals leads to measurement errors that are comparable in value to the signal under study.

The modern scientific “gold standard” for solving this problem is Lorentzian Curve Fitting (LCF) [1, 2]. In the simplest case, this method is based on iterative selection of the analytical Lorentzian function and its quantitative comparison with the received signal. After that, the maximum of the already perfectly scaled and shifted function is found. Currently, this problem is not solved so straightforwardly—LCF has many new optimized calculation methods. The algorithms of Lorentzian Curve Fitting include such methods as linear least squares method, described in detail in [3, 4], as well as the nonlinear method based on the Levenberg–Markwardt algorithm [5, 6]. Many of these methods have significantly increased the accuracy of measurements, but they have some drawbacks. The main one is rather high requirements for computing resources.

In this regard, the correlation methods recently presented in the literature, simple in software and hardware implementation, and therefore operating faster, have become a serious competitor to LCF. Separate attempts to compare the accuracy parameters of different methods were made in [7, 8], but there is no

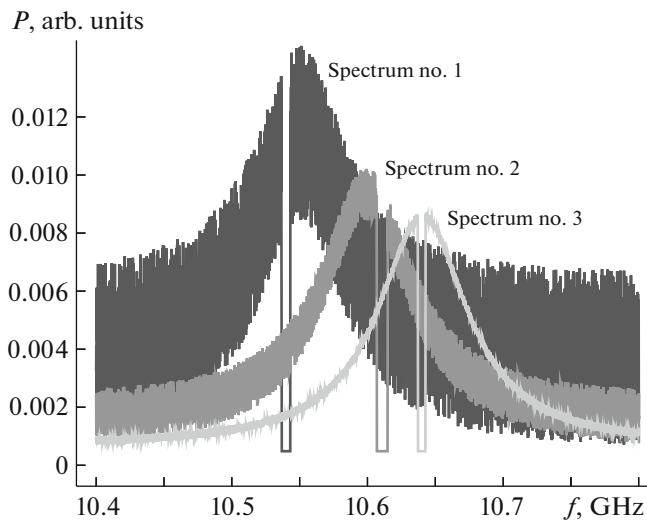


Fig. 1. Generated Brillouin spectra.

comprehensive analysis of this problem at the moment. In addition, experiments comparing the methods were conducted for different signals, and this is still unclear how the methods will behave in the same not “comfortable” conditions. Thus, the aim of this paper is to compare the accuracy of the backward correlation method and its classical analog in the conditions of extreme optoelectronic and digital noise.

SETTING UP A NUMERICAL EXPERIMENT

A set of spectra containing two types of defects was generated for the experiment. The first ones simulate the noise of the recorders and lead to a random variation from spectrum to spectrum of the signal-to-noise ratio in range from 2 to 20 dB. The second ones are digitization failures, which lead to the appearance of random by location and duration zeroed values of the discrete function. Such a discrete function can be expressed as follows:

$$P(f) = \left(P_N + \frac{W}{\pi} \left[\frac{1}{W^2 + f^2} \right] \right) \left[1 + \frac{(f - \mu) |f - \nu|}{(f - \nu) |f - \mu|} \right], \quad (1)$$

where μ is the frequency coordinate of the digital signal dip beginning; ν is the frequency coordinate of the digital signal dip end, and ν is always greater than μ and is set randomly within the useful signal of the spectrum; W is the scale coefficient of the spectral function responsible for the spectrum width and the amplitude of the useful signal; P_N is the noise component amplitude of signal.

The spectral component central frequency was also randomly set in the range of 10.55–10.65 GHz. Figure 1 shows three random spectra from the resulting sample. Mathematical processing was carried out further. The LCF method is widely presented in the literature and

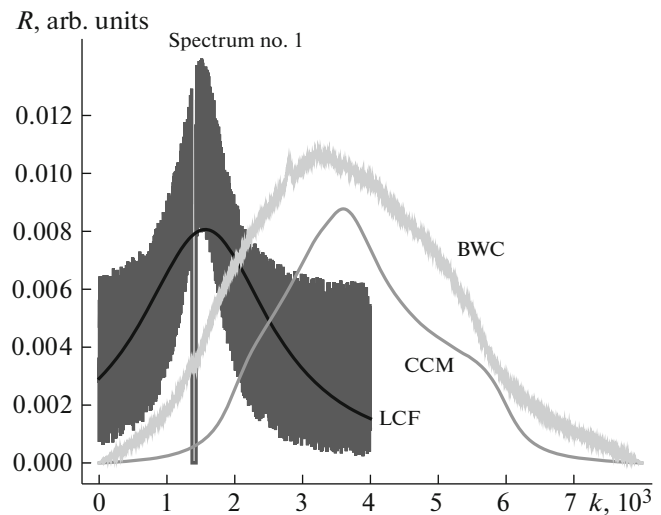


Fig. 2. The result of processing spectrum no. 1 by three methods. X-axis—counts.

is implemented using various algorithms described in detail in [9]. The traditional correlation method has also been well studied by various authors [10, 11]. Its cross-correlation function in continuous form is presented below:

$$R_c(f) = \int P(f)L(f - k)df, \quad (2)$$

where P is a function describing a given spectrum; L is a function describing an ideal Lorentzian spectrum; k is the value of the spectrum shift.

The backward correlation method developed by the authors earlier can be represented as:

$$R_b(f) = \int P(f)P'(f - k)df, \quad (3)$$

where P' is the original spectrum inverted along the frequency axis, shifted by k points.

It is obvious that the integration of functions (2) and (3) using Residue theorem in both cases will also give Lorentzian functions that have an identifiable and uniquely associated maximum with the desired value.

Figure 2 shows the result of processing the spectrum no. 1. The resulting spectra are given for the cross-correlation with the ideal Lorentzian curve (CCM—Cross-Correlation Method), as well as for the backward correlation (BWC—Backward Correlation) and LCF. The maxima of BWC and CCM are shifted to the right due to their algorithmic features.

As a result of processing the spectrum by the backward correlation method, one can notice a defect that occurs in the place where the original spectrum has a drop in the function to zero. This spike is due to the fact that when the spectra shift relative to each other at the moment of superposition of dips, the number of zero elements that sum up in the resulting function

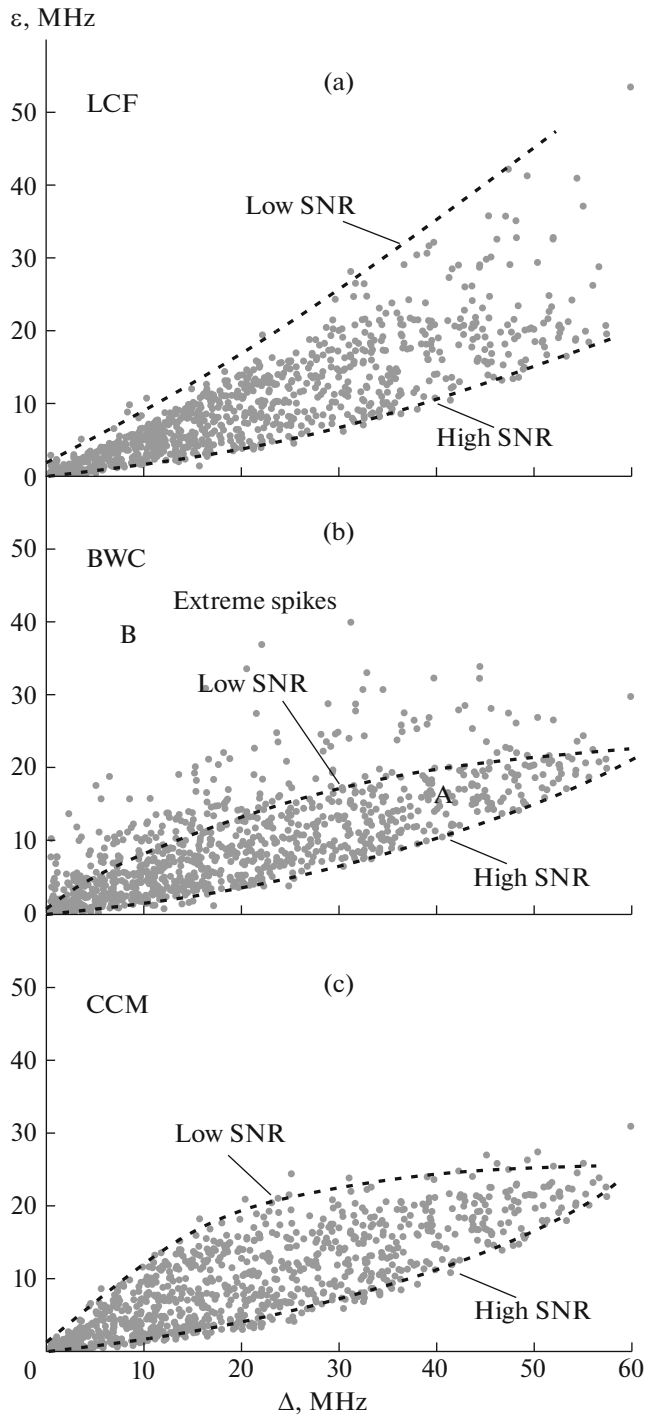


Fig. 3. The distribution of the Brillouin spectrum maximum finding errors for case no. 1; Δ is defined as $\nu - \mu$. A and B are more and less “dense” regions, respectively.

decreases, which leads to a spike in the value of the correlation function.

The artifact described in this paper and presented as a local zeroing of the function under study can be caused not only by digitization defects, but also by incorrect operation of the spectrum scanning algo-

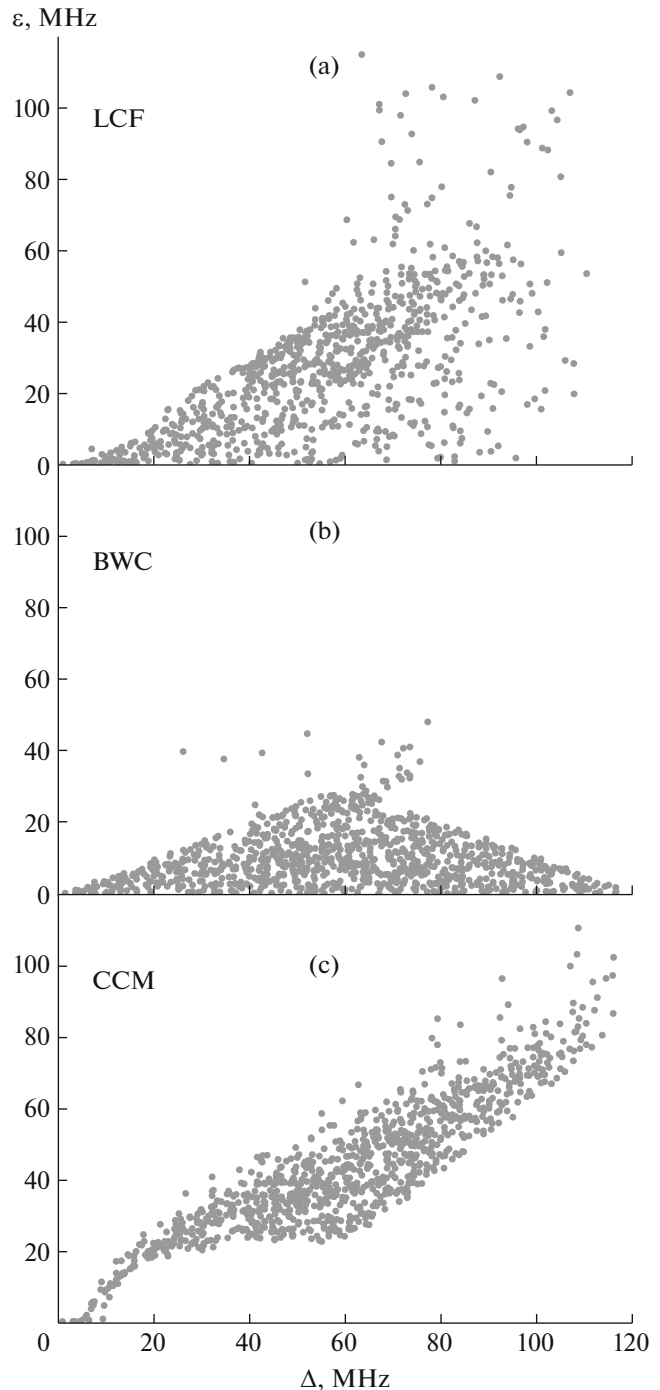


Fig. 4. The distribution of the Brillouin spectrum maximum finding errors for case no. 2; Δ is defined as $\nu - \mu$.

rithm. Its length and location in the spectrum can be completely different. Two cases are discussed below: the first one describes the appearance of such a defect in spectral regions that do not contain the desired maximum; the second one, on the contrary, assumes that the maximum frequency of the spectrum is always within the boundaries of the dip.

Table 1. Efficiency of finding the maximum of the Brillouin spectrum

Method	SNR, dB	BFS standard deviation, MHz		
		No artifact	Case 1	Case 2
LCF	<5	1.12	10.68	7893.28
	5–10	0.24	7.55	4076.74
	>10	0.04	6.19	316.42
BWC	<5	2.17	9.12	9.69
	5–10	0.74	6.18	7.53
	>10	0.14	5.83	7.68
CCM	<5	0.46	7.61	20.39
	5–10	0.19	6.54	19.51
	>10	0.09	6.37	16.13

RESULTS AND DISCUSSION

For each case of artifacts occurrence in the spectrum, one thousand spectra were generated.

To assess the effect of the artifact on the spectrum maximum finding error, three methods were used to construct the dependence of the error in determining the spectrum on the width of the artifact. Figure 3 shows the obtained dependencies for three methods: LCF, BWC, and CCM.

Such a significant spread of data on the obtained dependencies is due to variations in the signal-to-noise ratio (SNR). With a large amount of experimental data, the graphs allow one to clearly distinguish the area that characterizes the accuracy (here—the standard deviation) of determining the desired value from the lowest signal-to-noise ratio to the highest.

For the Lorentzian curve fitting method (Fig. 3a), these lines indicate a smooth increase in the detection error with dip width increase in all cases. At the same time, the difference of standard deviations increases steadily in the entire studied area at extremely low signal-to-noise ratios and practically noiseless signals, which looks quite logical and indicates the effectiveness of the Lorentzian curve fitting method at high signal-to-noise ratios and relatively small dip sizes.

Both correlation methods (Fig. 3b, 3c), as it is easy to see, produce data that resembles the form of hysteresis. At the same time, in the case of the backward correlation method (Fig. 3b), the object formed by this hysteresis can be conditionally divided into two parts: more and less “dense.”

In the more “dense” part, designated by the letter A, more points are concentrated, which means more measurements with corresponding higher accuracy. Region B has single but larger fluctuations, which are not typical for the classical cross-correlation method. Based on this, we can conclude that the backward correlation method is preferable here, provided that additional means of insurance against large deviations,

which can be cut off by the threshold algorithm, are used.

The data obtained for the second case (Fig. 4), when the dip is located in the region of the desired maximum, is largely similar to the situation described above, with the exception of some bends and local fluctuations. The backward correlation method revealed the following interesting features (Fig. 4b). First, there is a decrease in the standard deviation that is proportional to the previous growth, starting after the width of the spectral dip of 60 MHz. This feature suggests the possibility of using the method for processing spectra that are almost completely distorted by both noise and partial loss of information. Secondly, the lower part of the hysteresis in Fig. 4b practically “lies” on the frequency axis, which indicates a higher probability of obtaining an accurate result in the entire studied area.

Table 1 provides information on the effectiveness of all three methods at different signal-to-noise ratios. In each case, the spectra were divided into three groups according to the signal-to-noise ratio (SNR). The first group included spectra with low SNR (up to 5 dB), the second group with medium SNR (5–10 dB), and the third group with high SNR (>10 dB).

As noted above, the traditional method of approximation by the Lorentzian function is relatively effective at high signal-to-noise ratios if the dip does not fall on the desired central region of the spectrum. In other cases, correlation methods are more effective. At the same time, when the dip is in the peak region, the backward correlation method becomes the most effective; the classical correlation method shows slightly less accuracy; while the method of approximation by the Lorentzian function completely loses its relevance in such extreme conditions.

It is worth noting that in real monitoring systems based on the use of Brillouin scattering, the artifacts mentioned above are quite rare in commercial equipment, but can be detected during studies using the experimental set-ups. Undoubtedly, it is worth considering cases where the artifact appears in the spec-

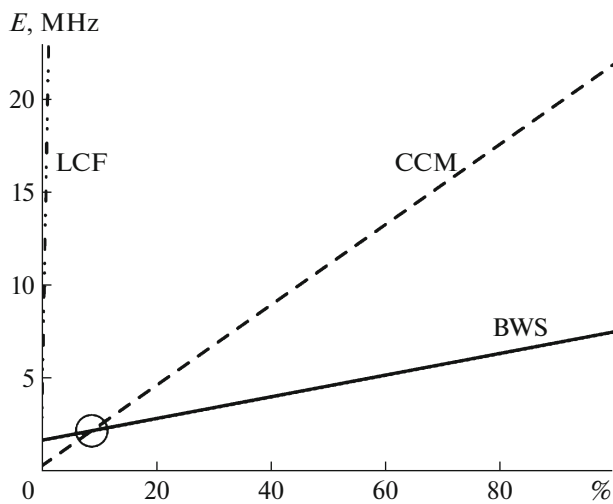


Fig. 5. The standard deviation of determining the BFS, depending on the probability of the artifact occurrence.

trum with some degree of probability. The predicted standard deviation E of the BFS measurement under conditions of artifact occurrence with probability P can be estimated approximately as follows:

$$E = E_0(1 - P/100) + E_a(P/100), \quad (4)$$

where E_0 is the standard deviation in the absence of artifacts; E_a is the standard deviation in the presence of an artifact.

As a result of calculating the system accuracy, the graphs presented in Fig. 5. According to these graphs, starting from the 9% probability of artefact occurrence (the area marked with a circle), the BWC method shows better results in the accuracy of determining the Brillouin spectrum maximum in comparison with the CCM method. Also, for a qualitative assessment of the efficiency of determining the Brillouin spectrum maximum, Fig. 5 shows a similar dependence for the LCF method.

CONCLUSIONS

The accuracy parameters of modern methods for detecting the Brillouin scattering peak in optical fibers are compared. For all existing signal-to-noise ratios, the LCF method demonstrates lower accuracy than both correlation methods. It is shown that the backward correlation method is more precise than the classical correlation method in the vast majority of cases.

The accuracy of the considered methods is estimated depending on the probability of artifacts appearing in the Brillouin scattering spectra. It is shown that when the 9% probability of artifact occurrence is exceeded, the BWC method shows better results than the other methods considered.

The BWC method can be potentially applied in applications such as temperature and strain discrimi-

nation in polarization maintaining fibers [12], where it is required to accurately separate the Brillouin spectra of two polarization axes of an optical fiber; distributed birefringence measurement in polarization maintaining fibers [7]. In addition, this method may have potential advantages in reflectometric study of non-standard optical fibers with high losses (i.e., active optical fibers [13]).

FUNDING

The work was performed as part of the State Assignment no. AAAA-A19-119042590085-2.

REFERENCES

1. Madsen, K., Nielsen, H.B., and Tingleff, O., *Methods for Non-Linear Least Squares Problems*, London: Informatics and Mathematical Modeling, Technical Univ. of Denmark, 2004.
2. Seber, G. and Wild, C.J., *Nonlinear Regression*, New York: Wiley, 2003.
3. Dhliwayo, J., Webb, D.J., and Pannell, C.N., *Proc. SPIE*, 1996, vol. 2838, p. 276. <https://doi.org/10.1117/12.259808>
4. DeMerchant, M., Brown, A.W., Bao, X., and Bremner, T.W., *Proc. SPIE*, 1998, vol. 3330, p. 315. <https://doi.org/10.1117/12.316987>
5. Levenberg, K., *Q. Appl. Math.*, 1944, vol. 2, no. 2, p. 164. <https://doi.org/10.1090/QAM/10666>
6. Fletcher, R., *A Modified Marquardt Subroutine for Non-linear Least Squares*, Technical Report AERE-R 6799, Harwell: Oxford Univ. Department, Theoretical Physics Division, 1971.
7. Barkov, F.L., Konstantinov, Yu.A., and Krivosheev, A.I., *Fibers*, 2020, vol. 8, no. 9, p. 60. <https://doi.org/10.3390/fib8090060>
8. Haneef, S.M., Yang, Z., Thévenaz, L., Venkitesh, D., and Srinivasan, B., *Opt. Express*, 2018, vol. 26, no. 11, p. 14661. <https://doi.org/10.1364/OE.26.014661>
9. Cheng Feng, Xin Lu, Preussler, S., and Schneider, T., *J. Lightwave Technol.*, 2019, vol. 37, p. 5231. <https://doi.org/10.1109/JLT.2019.2930919>
10. Farahani, M.A., Castillo-Guerra, E., and Colpitts, B.G., *IEEE Sens. J.*, 2013, vol. 13, no. 12, p. 4589. <https://doi.org/10.1109/JSEN.2013.2271254>
11. Farahani, M.A., Castillo Guerra, E., and Colpitts, B.G., *Opt. Lett.*, 2011, vol. 36, no. 21, p. 4275. <https://doi.org/10.1364/OL.36.004275>
12. Barkov, F.L., Konstantinov, Yu.A., Burdin, V.V., and Krivosheev, A.I., *Instrum. Exp. Tech.*, 2020, vol. 63, pp. 487–493. <https://doi.org/10.1134/S0020441220040223>
13. Belokrylov, M.E., Konstantinov, Yu.A., Latkin, K.P., Claude, D., Seleznev, D.A., Stepin, A.A., Konin, Yu.A., Shcherbakova, V.A., and Kashina, R.R., *Instrum. Exp. Tech.*, 2020, vol. 63, pp. 481–486. <https://doi.org/10.1134/S00204412200500129>